J. Phys. II France **7** (1997) 1099–1109 AUGUST **1997**, PAGE 1099

Collective Diffusion of "Living Polymers"

A. Ott ([1,2,*]), J.P. Bouchaud ([1,3]), W. Urbach ([1]) and D. Langevin ([1])

([1]) École Normale Supérieure, Laboratoire de Physique Statistique ([**]), 75005 Paris, France
([2]) Institut Curie, Laboratoire de Physico Chimie Curie ([***]), 75231 Paris, France
([3]) Service de Physique de l'État Condensé, Centre d'Études de Saclay, Orme des Merisiers, 91191 Gif-sur-Yvette Cedex, France

(Received 5 November 1996, revised 24 March 1997, accepted 5 May 1997)

PACS.68.35.Fx – Diffusion; interface formation
PACS.61.25.Hq – Macromolecular and polymer solutions; polymer melts; swelling
PACS.82.70.-y – Disperse systems

Abstract. — We have studied the "collective" diffusion of a concentrated solution of "living polymers" in brine, which in certain concentration conditions exhibit superdiffusive (Lévy flight) behaviour when tracer diffusion is considered. The concentration profile of the diffusion front is monitored over time using a Michelson interferometer. We show how a concentration dependent diffusion constant can be extracted from the fringe pattern. We find that the diffusion constant decreases linearly with increasing concentration, at variance with a power-law dependence, expected when the interaction between chains is neglected.

1. Introduction

Cylindrical micelles have been studied as a model system for living polymers, *i.e.* flexible macromolecules that may break and recombine. Numerous techniques, among these light and neutron scattering [1], electron microscopy [2], NMR [3], t-jump and p-jump [4] and also fringe pattern fluorescence recovery after photobleaching have been used. Using this latter technique we showed that these micelles indeed are transient objects, *i.e.* they break and recombine on ms to 100 ms timescales [5,6]. The measured monomer self-diffusion constants can be explained by a combination of polymer reptation and changes of track due to breakage and recombination [7]. Our experiments further revealed an interesting anomalous diffusion behaviour, which we interpreted in terms of Lévy-flights [8,9] an explanation arising almost naturally from the large size distribution of these micelles, and the strong dependence of the diffusion constant as a function of the size of the micelle. Finally, the temperature dependence of the self-diffusion constant at high concentrations is well-related to the amount of energy to form a micelle endcap, as measured by other techniques [10].

An unsolved problem (from an experimental point of view) remains the size distribution of these objects: due to the transient character of these concentration dependent objects a direct

(*) Author for correspondence (e-mail: Albrecht.Ott@Curie.fr)
(**) Associé au CNRS et aux universités Paris 6 et 7
(***) UMR 168 du CNRS, associé à l'université Paris 6

measurement of their size is not possible. However, the shape of this distribution (in particular for small sizes) was one of the input of the Lévy flight interpretation proposed in [8,9], the other one being the dependence of the diffusion constant on the size; it would thus be gratifying to obtain independent confirmation of these assumptions. Recent numerical simulations have been published [11], and provide interesting informations.

In this paper we present a new approach to study the collective diffusion of these micelles in a Michelson interferometer. Collective diffusion [12] is *a priori* very different from self diffusion (or tracer diffusion) [13], although they coincide in the dilute limit. This is particularly clear in the case of a semi-dilute polymer solution: at short time scales as in a light scattering measurement collective diffusion is related to breathing of the network, and is thus accelerating with concentration. Conversely, self diffusion becomes slower and slower. For a semidilute polymer solution scaling arguments lead to a power of $\phi^{9/4}$ for the osmotic pressure as a function of concentration ϕ and to a power of $\phi^{3/4}$ for the collective diffusion constant [14] as compared to $\phi^{-7/4}$ for self-diffusion. Collective diffusion of polymers has been measured by forced Rayleigh scattering [15]. However the situation is different when considering cylindrical micelles: Constraints may relax by breakage and recombination. More importantly, the size distribution of these objects is large and their mean length increases with concentration.

Starting with a sharp interface between a high concentration and a low concentration region, we expect to observe a highly asymmetrical diffusion profile, allowing us to extract a concentration depend diffusion constant $D(\phi)$. This diffusion constant can be related to the concentration dependent size distribution of these micelles, and not (in a first approximation) to the size dependence of the diffusion constant of each micelle. Simple arguments give that $D(\phi)$ should first decrease as a power law $\phi^{-\gamma}$ as ϕ is increased, with a rather large value of γ, and then increase when interactions between chains become dominant. Although our experimental data are not incompatible with $\gamma \simeq 0.6$ a simple linear decrease $D(\phi) = D_0 - D_1\phi$ is a very good description for ϕ between 0 and 100 mM.

2. Experimental

Cylindrical micelles were made of cetyltrimethylammoniumbromide (CTAB) from Aldrich solubilized without further purification in brine made of KBr in water at concentrations of 0.5, 1, and 2 M. Experiments were performed at 40 °C. At this temperature only the 2 M sample remained noticeably viscoelastic. Half the volume of a Hellma quartz cuvette, size of $20 \times 10 \times 0.2$ mm, was filled with 100 mM CTAB solution. To avoid a curved meniscus due to wetting forces and solution sticking to the glass walls of the empty half of the cuvette, it was spun with the Hellma centrifuge leading to a perfectly clean and straight interface after only a few minutes. The upper half of the cuvette was then filled with brine and the cuvette was quickly inserted into the pathway of a standard Michelson interferometer as used for teaching courses, illuminated with a sodium lamp and an interference filter selecting the 590 nm band. The interference pattern was projected onto a Sony CCD camera equipped with standard zoom optics plus an additional biconvex lens. Resolution due to optics limitations and camera was about 40 microns. The image was transferred to a Macintosh II ci computer equipped with a frame grabber and NIH Image software leading to a distance of 12 microns per pixel or roughly 10 mm per image. The software was modified in a way that one line of the live image perpendicular to the diffusion front could be chosen. This line was then grabbed at suitable time intervals and a new image was constructed by adding these lines one by one showing the time evolution of the diffusion front (Fig. 1).

Attention had to be given to the orientation of the cuvette inside its temperature controlled housing (see Fig. 2), since gravitational effects could not be neglected: a vertical orientation but

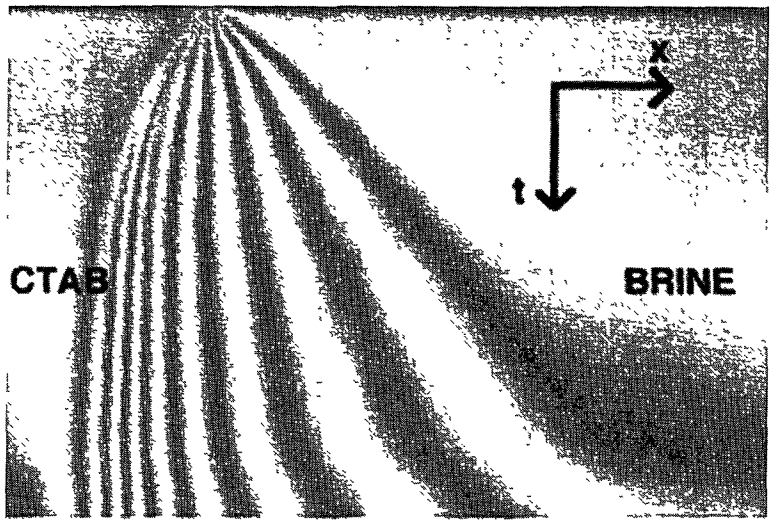

Fig. 1. — Evolution of interference fringes as a function of time (vertical axis) for a horizontally oriented cuvette at 0.5 M KBr. Total observation time is 2.5 hours.

with the CTAB at the bottom leads to a regular pattern as a signature of an instability at the interface. Horizontal orientation of the cuvette did lead to a stable interface, but the diffusion constant derived from glycerol as a test substance turned out to be much higher than expected and results for this orientation have to be considered cautiously, since the interface presumably tilts. Only when the dense liquid was at the bottom the diffusion constant for glycerol matched the literature values. This is thus the geometry on which we will focus, although some results concerning the horizontal orientation will be reported. The longest measurement took 9 hours at highest salinities. Note that even after 16 hours the diffusion front was still perfectly regular (Fig 3).

Note finally that no traces of wetting or flow are seen in the cuvette when it is inserted in the interferometer. This is not surprising since our system is an amphiphilic system. Even after centrifugation the surfaces of the upper part of the cuvette must still be covered with surfactant. The surface tension between the glass, brine and CTAB is therefore expected to be very low and capillary effects, given further the high viscosity of the CTAB solution, can certainly be neglected.

3. Image Analysis and Diffusion Constant

Images were analyzed using Kaleidagraph software. The concentration profile was extracted from the interference pattern of the interferometer, supposing the light pass difference proportional to concentration, 100 mM of CTAB corresponding to nine wavelengths. It was found that interference fringes sometimes had a slight tendency to creep, probably due to room temperature fluctuations during the observation. For this reason only the shape of the concentration profiles could be extracted and not the absolute values of the concentration profile. We noticed that at the beginning of the experiment interference fringes spacing was modified due to the relatively strong refraction index gradient at the interface, these profiles had to be regarded with caution. Due to this limitation a reasonable calculation of the profile could be achieved for a factor of five to 15 in observation time only.

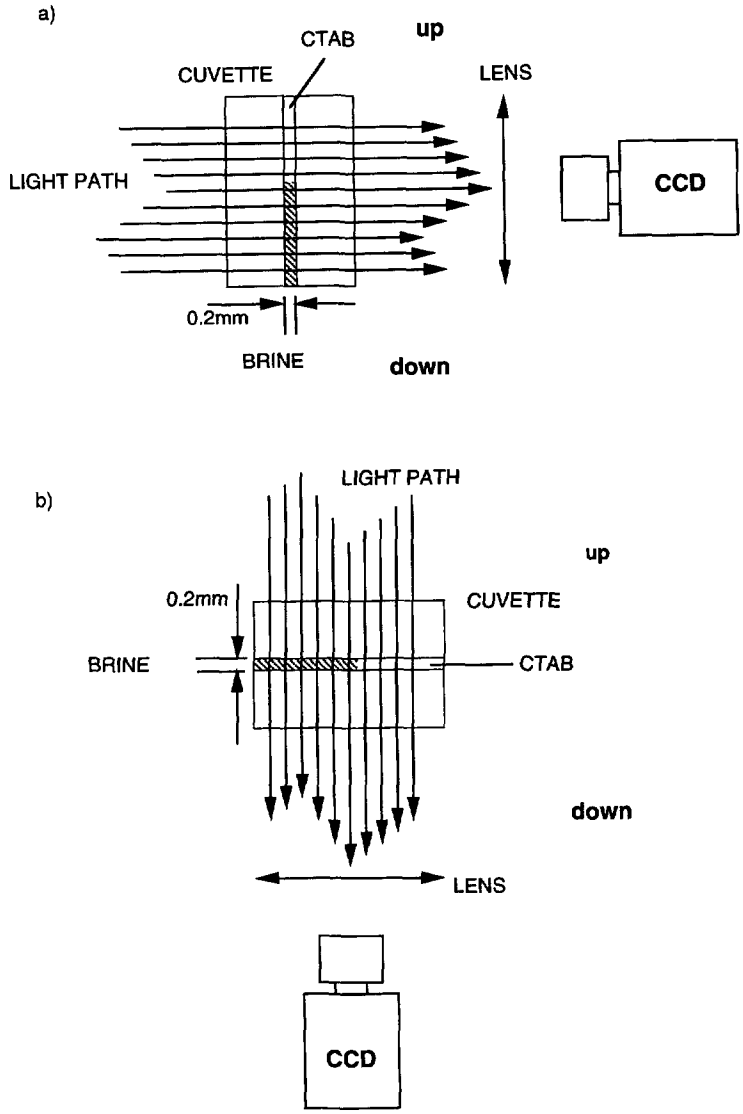

Fig. 2. — Scheme of the orientation of the cuvette during the experiment: a) vertically oriented cuvette, b) horizontally oriented cuvette. Components belonging to the interferometer or to temperature control are not shown.

We suppose that the basic diffusion equation takes the following form:

$$\frac{\partial \phi(x,t)}{\partial t} = \frac{\partial}{\partial x}\left[D(\phi)\frac{\partial \phi(x,t)}{\partial x}\right] \tag{1}$$

where x denotes the distance from the initial interface, t is the time and $D(\phi)$ the concentration dependent diffusion constant. In principle, $D(\phi)$ can thus be extracted from the images by

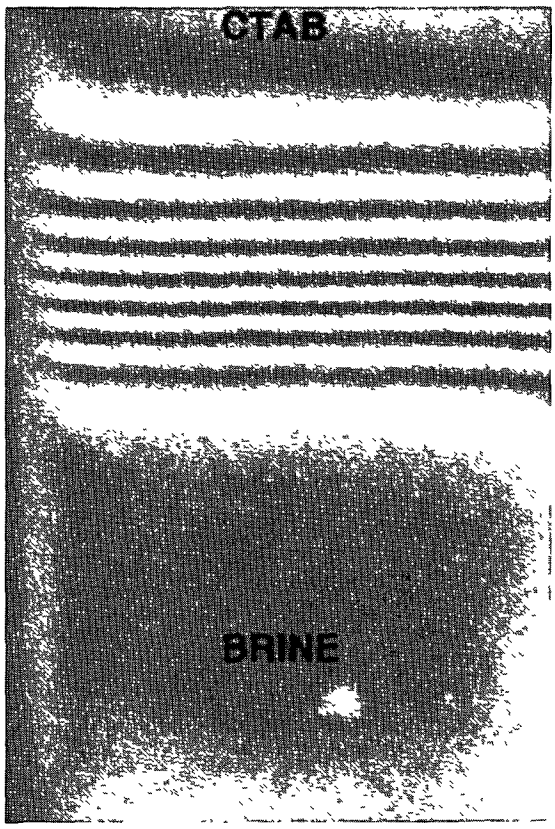

Fig. 3. — Interference fringes after a diffusion time of 16 hours. Note that the diffusion profile is still perfectly regular (vertically oriented cuvette).

calculating

$$D(\phi) = \frac{\int^{x(\phi)} \mathrm{d}x' \frac{\partial \varphi(x',t)}{\partial t}}{\frac{\partial \phi(x,t)}{\partial x}|_{\phi}} \tag{2}$$

To simplify the computation of the concentration dependent diffusion constant it was checked that the profiles at different observation times were to a good approximation self-similar (Fig. 4). In other words, that an exponent ν could be found so that the diffusion profile is described by a reduced variable: $\phi(x,t) = \varphi(u = \frac{x}{t^{\nu}})$. Figure 4a gives diffusion profiles at different times of observation, Figure 4b shows the superposition of the same curves stretched by a factor t^{ν}. Exponents ν were close to 0.5, although slightly smaller, at least in the vertical case ($\nu = 0.41$ for the 1 M KBr and $\nu = 0.38$ for 0.5 M KBr). This could be due to gravity effects, which slightly slow down diffusion through a buoyancy term that we have neglected in equation (2).

For self similar diffusion profiles the diffusion constant is given by a much more convenient expression:

$$D(\varphi) = -\frac{\nu}{t} \frac{\int^{\varphi} \mathrm{d}\varphi u(\varphi)}{\frac{\partial \varphi}{\partial u}|_{\varphi}} \tag{3}$$

The derivative term can be directly calculated; in order to diminish its noise a running average

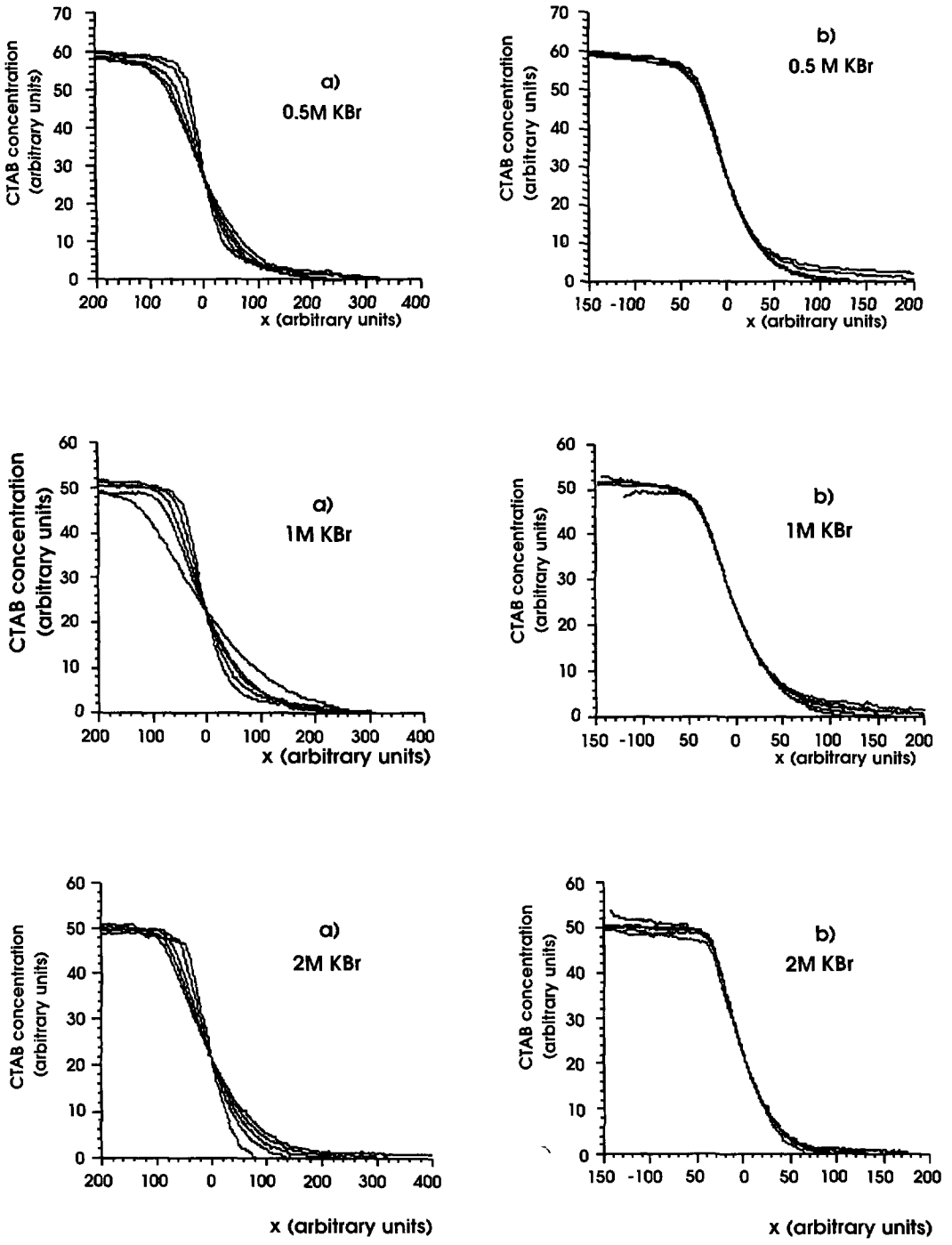

Fig. 4. — Concentration profiles for a vertically oriented cuvette. From top to bottom: 0.5 M, 1 M and 2 M KBr; a) profiles at different times (a factor of 5 to 15 between the shortest and the longest observation time). b): Superposition of these profiles after stretching with t^{ν}. ν is 0.38, 0.45 and 0.5 for 0.5, 1 and 2 M KBr respectively.

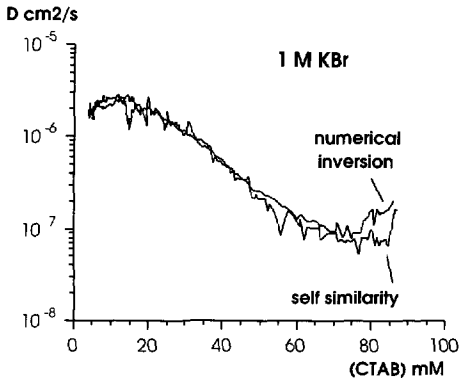

Fig. 5. — Plot of the concentration dependent diffusion constant for a horizontally oriented cuvette filled with 1 M KBr calculated using self similarity (Eq. (3)) or calculated by numerical inversion of the diffusion equation (Eq. (2)) around the same observation times (both curves superposed on a semi-log plot).

was applied. A suitable window was ten pixels in the middle of the profile and 50 pixels at both ends where the slope was weak. Since the shape of the integral term is very sensitive to noise in concentration values far from the interface, its naive calculation very often lead to an important offset. Another difficulty in the calculation of the integral was that the precise location of the initial boundary between the liquids was *a priori* not so well-defined. It was not simply taken from an image of the interference pattern (Fig. 1) since its position might be shifted at the beginning of the experiment due to the already mentioned refraction effects. A first control of the integral offset was given by directly looking at its shape: curvature had to be increasingly concave far from the interface. At points where the slope remained constant, side effects like uneven illumination became dominating and at these points the integral should be close to zero. We further assumed the diffusion constant to be well-behaved and a divergence of the diffusion constant at low $\frac{\partial\phi(x,t)}{\partial x}$ had to be due to either a wrong position of the interface (divergence at one end) or to a wrong offset (divergence at both ends). Note that $\frac{\partial\phi(x,t)}{\partial x}$ can become very small which makes this iterative approximation very precise. Following this method the interface could be determined with a precision of about ± 1 or ± 2 pixels depending on the individual measurement. Its position always turned out to be in agreement with the initial guess from the image of the interference pattern. Note that the value of the integral at the interface and also the value of the derivative at this point have to scale with the same exponent ν as a function of time giving a further possibility of controlling of the calculation. Self similarity further means that concentration at the interface is constant. simplifying the adjustment of the offset of the concentration. This was simply done by superposing the curves and estimating their zero by eye. This was precise to a few mM of CTAB concentration.

We have finally checked directly, in the case of the (horizontally oriented) 1 M KBr sample, that the direct calculation using equation (2) gives very similar results to those obtained using a self-similarity assumption equation (3) – see Figure 5.

4. Results and Discussion

4.1. Vertical Orientation of the Cuvette, CTAB above Brine. — *The diffusion* constant as a function of concentration can be seen in Figure 6, and is well-approximated by a

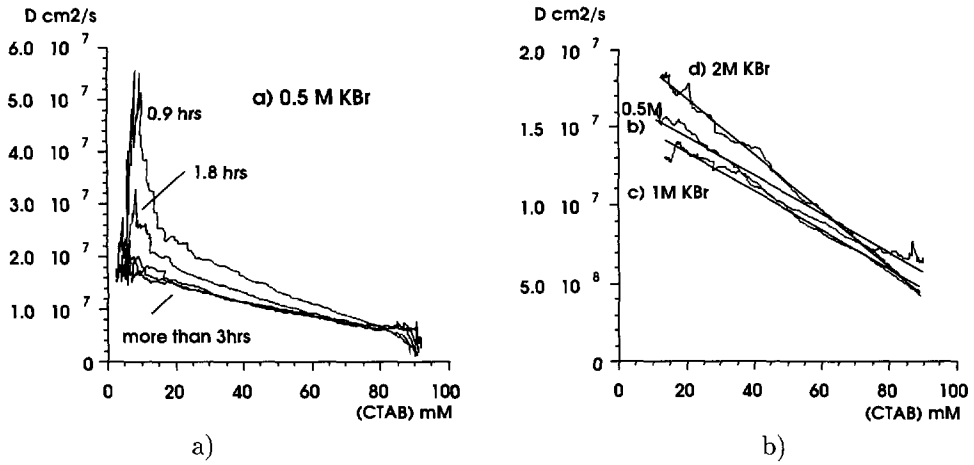

Fig. 6. — Concentration dependent diffusion constant for 0.5 M, 1 M and 2 M KBr vertically oriented, showing a linear dependence. a) 0.5 M for different observation times, between 0.9 and 7.2 hours. b)-d) linear regression of the $D(\phi)$ dependence at 0.5, 1 and 2 M KBr. Values for D_0 at zero concentration are 1.7, 1.6 and 2.0×10^{-7} cm^2/s respectively and slopes D_1 are 1.3 and 1.3 and 1.7×10^{-9} cm^2/s/mM.

simple linear relation $D(\phi) = D_0 - D_1\phi$ up to the highest concentrations $\phi = 100$ mM (but see the discussion below). Of course, this linear relation must break down for higher concentrations since $D(\phi)$ cannot become negative. Physically, interaction effects are expected to increase D at higher concentration.

We note that for different observation times t the diffusion constants extracted using (3) are very close which is consistent with the assumption of self similarity. At the lowest concentrations, the measured values agree well with our previous self-diffusion study (D_0 around 2×10^{-7} cm^2/s), which is another check of the consistency of our procedure.

It is interesting to see that the values for D are about the same for the three concentrations of KBr. Self diffusion measurements also gave roughly similar values. Note however that D seems to be minimum for 1 M KBr; this might be related to the fact that the rheological relaxation time reaches a maximum for 1.5 M KBr [16], a fact which could be induced by the branching of the micelles.

4.2. Horizontal Orientation of the Cuvette. — The 0.5 M KBr and the 1 M KBr samples also gave self-similar concentration profiles, but not the 2 M KBr sample. The "effective" diffusion constant extracted as above as a function of concentration seems to depart from a linear concentration dependence (which holds in the vertical case) evolving towards an exponential or a power-law (see Fig. 5). Note however that the diffusion constant in the horizontal case is an order of magnitude higher than for the vertical setup, showing that gravity enhances mixing of the liquids. We conclude that we probably see here a tilting of an interface of two liquids with different densities, and not a simple diffusion front.

4.3. Theory. — Since we observe that the diffusion constant *decreases* with concentration in the studied regime ($\phi \leq 100$ mM), it is not unreasonable to start by neglecting completely the (repulsive) interaction between the micelles, while still retaining the breakage/recombination processes. In the present experimental situation, we estimate the breakage/recombination time to be of the order of $\tau_b \simeq 100$ ms [9,17], to be compared to the time scale for diffusion, which

is of the order of hours. We can thus make an "adiabatic" approximation, assuming that the size distribution $P(\ell, \phi)$ (ℓ is the length of the micelles) always sticks to its equilibrium form, which we will take, following [8,9] to be:

$$P_{\rm eq}(\ell, \phi) = \mathcal{N} \ell^{-2\sigma} \exp[-\frac{\ell}{L(\phi)}] \tag{4}$$

where $L(\phi)$ is the typical size of the micelle for a given concentration ϕ $P(\ell, \phi)$ is the probability (per unit volume) to find a micelle of length ℓ. Hence, one should have by definition:

$$\phi = \int_0^\infty {\rm d}\ell \; \ell P(\ell, \phi) \tag{5}$$

leading to $L(\phi) \propto \phi^{\frac{1}{2(1-\sigma)}}$ The simplest, mean-field case corresponds to $\sigma = 0$ and $L(\phi) \propto \sqrt{\phi}$ [7]. Recent numerical simulation [11] support equation (4), although the sign of σ is found to be *negative*, at variance with what was surmised in [8,9] (but in agreement with theoretical calculations [18]). Note however that equation (4) with $\sigma > 0$ was only chosen to describe the possibility of an excess probability of very small, fast micelles. This is actually what the numerical simulations of [11] show. In other words, equation (4) with $\sigma < 0$ does not describe well $P_{\rm eq}(\ell, \phi)$ for very small ℓ's.

Now, we assume that the diffusion constant of a micelle of size ℓ is given, in the semi-dilute regime (corresponding in our experiment to $\phi > 10$ mM) by a generalized reptation law [8,9]:

$$\begin{aligned} \mathcal{D}(\ell) &= \frac{\mathcal{D}(a) a}{R(\ell)} && \ell < g_{\rm e} \\ &= \frac{\mathcal{D}(a)}{\xi} \left(\frac{g_{\rm e}}{\ell}\right)^\beta && \ell > g_{\rm e} \end{aligned} \tag{6}$$

where a is the size of the "monomer" (the smallest spherical micelle) and $D(a)$ its associated Stokes diffusion constant, and $R(\ell)$ the radius of gyration of a micelle of size ℓ. $g_{\rm e}$ is the entanglement length, and β an exponent which is equal to $\beta = 2$ in the usual reptation picture. In our experimental situation where the salt concentration is high, we have estimated $L(\phi)$ to be of the order of 100 persistence lengths; this means that a substantial fraction of chains indeed move by reptation, which is important to observe a Lévy flight regime). However, as we shall see below, we expect that short chains (such that $\ell < g_{\rm e}$) give the dominant contribution for collective diffusion; the value of β thus cannot be reached by this method.

There are *a priori* three times scales of importance: the breakage/recombination time scale $\tau_{\rm b}$, the ℓ dependent reptation time $\tau_{\rm r}$, and the experimental diffusion time t. Since, as expected, the collective diffusion constant is dominated by the contribution of the smallest micelles, we shall argue that the relevant regime of time scales is $\tau_{\rm r} \ll \tau_{\rm b} \ll t$. (Actually, precisely the same condition is needed for the very existence of a Lévy flight regime [9]). In this limit, the diffusion equation for a the concentration of a given "specie" of micelle is given by:

$$\frac{\partial P(\ell, \phi, x)}{\partial t} = -\{\ell \to \ell'\} + \{\ell' \to \ell\} + \frac{\partial}{\partial x} \mathcal{D}(\ell) \frac{\partial P(\ell, \phi, x)}{\partial x} \tag{7}$$

where we have written symbolically the terms corresponding to breakage and recombination, but which cancel each other according to our "adiabatic" ($\tau_{\rm b} \ll t$) assumption. Multiplying by ℓ the above equation and integrating over ℓ and using the explicit form of $P_{\rm eq}$, we find:

$$\frac{\partial \phi}{\partial t} \propto \mathcal{D}(a) \frac{\partial}{\partial x} \left[\phi^{\frac{2\sigma-3}{2(1-\sigma)}} \left(\int_a^{g_{\rm e}} \frac{{\rm d}\ell}{R(\ell)} \ell P_{\rm eq}(\ell, \phi) + \int_{g_{\rm e}}^\infty \frac{{\rm d}\ell}{\xi} \left(\frac{g_{\rm e}}{\ell}\right)^\beta \ell P_{\rm eq}(\ell, \phi) \right) \frac{\partial \phi}{\partial x} \right]. \tag{8}$$

It is easy to see that the last integral is in general governed by its lower bound, which means that the major contribution to the diffusion constant comes from the smallest micelles. Therefore, both integrals give the same contributions (up to prefactors), and we find:

$$D(\phi) \propto \mathcal{D}(a)\ \frac{g_e^{3-2\sigma}}{\xi}\phi^{\frac{2\sigma-3}{2(1-\sigma)}} \tag{9}$$

Using the standard scaling forms of g_e and ξ with ϕ [14], we thus finally find:

$$D(\phi) \propto \phi^{-\gamma} \qquad \gamma = -\frac{\zeta + 2\sigma - 3}{3\zeta - 1} - \frac{2\sigma - 3}{2(1-\sigma)} \tag{10}$$

where ζ describes the conformation of the chains within one "blob" (ideal, swollen, or stretched). Note that the exponent β indeed disappears from the computation, provided it is large enough so that the second integral above is dominated by its lower bound. In any case, γ is found to be larger than 2.41, for any value of σ (positive or negative). In other words, the above arguments show that in the semi-dilute regime where Lévy flight effects are observed (which implies that $g_e < L(\phi)$ [8,9]), the decay of the collective diffusion constant as a function of concentration should be very rapid. A rather unconvincing power-law fit of our data in the region $\phi = 10 - 100$ mM gives however $\gamma \simeq 0.6$, which is incompatible with equation (10). This suggests that osmotic pressure effects, although still too weak to *increase* $D(\phi)$ compared to D_0, contribute significantly, and (unfortunately) prevent us from extracting the information on σ which we hoped for.

5. Conclusion

We have thus shown in this paper how in principle fringe patterns could be used to extract reliable information on the collective, concentration dependent, diffusion constant of amphiphilic molecules. Although one motivation of our study was the theoretical possibility of obtaining directly some information on the size distribution of these objects, our experimental results are not in agreement with our expectations. We have at present no interpretation of the apparent linear decrease of the (collective) diffusion constant as a function of density; it might be that several competing mechanisms contribute in the region which we have investigated.

Acknowledgments

We would like to thank O. Cardoso for modifying the NIH-image software, C. Lemaire for fruitful discussions and O. Thoumine for critical reading of the manuscript.

References

[1] Candau S.J., Hirsch E., Zana R. and Adam M., *J. Coll. Inter. Sci.* **105** (1985) 521; *J. Phys. France* **45** (1984) 1263.
[2] Clausen T.M., Vinson P.K., Minter J.R., Davis H.T. and Miller G., *J. Phys. Chem.* **96** (1992) 474.
[3] Shikata T., Hirata H. and Kotaka T., *Langmuir* **5** (1989) 398.
[4] Candau S.J., Merikhi F., Waton G. and Lemarechal P., *J. Phys. France* **51** (1990) 977.

[5] Messager R., Ott A., Chatenay D., Urbach W. and Langevin D., *Phys. Rev. Lett.* **60** (1988) 1410.
[6] Ott A., Urbach W., Langevin D., Schurtenberger P.. Scartazzini R. and Luisi P., *J. Phys. C* **2** (1990) 5907.
[7] Cates M.E., *Macromol.* **20** (1987) 2289; *J. Phys. France* **49** (1988) 1593.
[8] Ott A., Bouchaud J.P., Langevin D. and Urbach W., *Phys. Rev. Lett.* **65** (1990) 2201.
[9] Bouchaud J.P., Ott A., Langevin D. and Urbach W., *J. Phys. II France* **1** (1991) 1465.
[10] Ott A., Morie N., Bouchaud J.P., Urbach W. and Langevin D., *J. Phys. IV France* **3** (1993) 91; Khatory A., Kern F., Lequeux F., Appel J., Porte G., Morie N., Ott A. and Urbach W., *Langmuir* **9** (1993) 933.
[11] Rouault Y. and Milchev A., *Phys. Rev. E* **55** (1997) 2020 and private communication.
[12] Batchelor G.K., *J. Fluid Mechanics* **74** (1976) 1.
[13] Chatenay D., Urbach W., Messager R. and Langevin D., *J. Chem. Phys* **86** (1987) 2343; Urbach W., Hervet H. and Rondelez F., *J. Chem. Phys.* **83** (1985) 1877.
[14] de Gennes P.G., Scaling Concepts in Polymer Physics (Cornell University Press, 1985).
[15] Léger L., Hervet H. and Rondelez F., *Macromolecules* **14** (1981) 1732.
[16] Khatory A., Lequeux F. and Kern F.. *Langmuir* **9** (1993) 1456.
[17] Cates M.E. and Candau S.J., *J. Phys. Cond. Mat.* **2** (1990) 6869.
[18] Schaefer L., *Phys. Rev. E* **46** (1992) 6061.